RESEARCH ARTICLE

Efficient Flatness Based Energy Management Strategy for Hybrid Supercapacitor/Lithium-ion Battery Power System

SALAM J. YAQOOB[1], **SEYDALI FERAHTIA**[2], **ADEL A. OBED**[3], **HEGAZY REZK**[4,5],
NASEER TAWFEEQ ALWAN[6,7], **HOSSAM M. ZAWBAA**[8,9,10], **AND SALAH KAMEL**[11]

[1]Department of Research and Education, Authority of the Popular Crowd, Prime Minister, Baghdad 10001, Iraq
[2]Laboratore d' Analyse des Signaux et Systemes, Department of Electrical Engineering, University of M'sila, M'sila 28000, Algeria
[3]Electrical Engineering Technical College, Middle Technical University, Baghdad 10001, Iraq
[4]Department of Electrical Engineering, College of Engineering in Wadi Alddawaseir, Prince Sattam Bin Abdulaziz University,
Wadi Alddawaseir 11942, Saudi Arabia
[5]Faculty of Engineering, Minia University, Minia 61519, Egypt
[6]Renewable Energy Research Unit, Technical College of Engineering, Northern Technical University, Kirkuk 3601, Iraq
[7]Department of Nuclear and Renewable Energy, Ural Federal University, Yekaterinburg 620002, Russia
[8]Faculty of Computers and Artificial Intelligence, Beni-Suef University, Beni-Suef 62521, Egypt
[9]CeADAR Irelands Center for Applied AI, Technological University Dublin, Dublin, D07 EWV4, Ireland
[10]Applied Science Research Center, Applied Science Private University, Amman 11931, Jordan
[11]Electrical Engineering Department, Faculty of Engineering, Aswan University, Aswan 81542, Egypt

Corresponding authors: Salam J. Yaqoob (engsalamjabr@gmail.com) and Hossam M. Zawbaa (hossam.zawbaa@gmail.com)

ABSTRACT This article offers a flatness theory-based energy management strategy (FEMS) for a hybrid power system consisting of a supercapacitor (SC) and lithium-ion battery. The proposed FEMS intends to allocate the power reference for the DC/DC converters of both the battery and SC while attaining higher efficiency and stable DC bus voltage. First, the entire system model is analyzed theoretically under the differential flatness approach to reduce the model order as a flat system. Second, the proposed FEMS is validated under different load conditions using MATLAB/Simulink. Thus, this FEMS provides high-quality energy to the load and reduces the fluctuations in the bus voltage. Moreover, the performance of the FEMS is compared with the load following (LF) strategy. The obtained results show that the proposed FEMS meet the real load power under fast variations with good power quality compared to the classical LF strategy, where the maximum overshoot of the bus voltage is 5%.

INDEX TERMS Hybrid power system, supercapacitor, Li-ion battery, flatness control theory, energy management system.

I. INTRODUCTION

Recently, the hybrid power system (HPS) has become an attractive solution to expanding threats of the global energy crisis and environmental pollution. The HPS is composed of several power sources with control of their operation using power electronics converters. Also, more advantages can be found using HPS, especially in electric vehicles (EVs) applications [1], [2], [3]. Moreover, the research gaps in this interesting field for energy management, control theory, and

The associate editor coordinating the review of this manuscript and approving it for publication was Shiwei Xia.

hybridization are being studied and developed to guarantee lower greenhouse gas emissions [4], [5], [6], [7]. In recent years, the HPS consisted of a supercapacitor (SC)/ lithium-ion battery hybrid energy storage system to realize a simple, reliable, and robust approach to mitigate battery stress-related impacts on performance, hence making it more desirable for direct-current (DC) grids or off-grid systems. The high energy density of the lithium-ion battery means issues can arise from the high battery current and high charge/discharge rate that may impact the system's stability. Therefore, this problem can be avoided using the SC, which supplies the required power to regulate the DC load voltage during transient operation

or sudden load changes [8]. To improve their performance and increase the system efficiency, hybridizing these sources is considered to protect them from temperature shocks or a lack of state of charge (SOC) control of the battery [9], [10], [11], [12]. Another advantage of using the SC is to alleviate the high-frequency system disturbances and fluctuation of current flowing in/out of the battery that affects the longevity of the battery. As a result, addressing these problems is by using a suitable energy management strategy (EMS) [13], [14], [15]. Also, the rate of fuel consumption and system efficiency are the main factors indicating the performance of the power system.

The well-known economic and environmental advantages, as well as advancements in technological innovations and achievements in semiconductor engineering have led to an upward trend in the adoption of EVs instead of the traditional vehicles that depend on internal combustion engines [15]. This has become more necessary due to the growing negative effects of greenhouse gases on the environment as a result of the use of fossil fuels [16], [17]. An ambitious plan to limit the rate of global warming increase to below 2 °C has been agreed upon in December 2015 by some 195 countries around the world at the Paris climate conference (COP21). This cannot be achieved in the said period if the transport sector is not fully involved [18]. As a result, hybrid electric vehicles (HEVs) have, in recent times, gained much attention and interest among manufacturers, researchers, and other stakeholders ever since it started entering the automotive industry on a large scale. The HEV technology has been in the automotive market since the 18th century. However, it started achieving a remarkable breakthrough in the industry in the 20th century [19]. The hydrogen fuel cell vehicle (HFCV) has a powertrain that is more complicated than that of the traditional vehicles, in that it generally contains at least two sources of energy, i.e., energy storage system (ESS) and fuel cell (FC), which for instance, involves an SC or a metal-ion lithium battery. It is important to optimize both the EMS and parameter sizing of the components [20]. The two key advantages due to fuel cells relative to internal combustion engines are: zero gas emissions and higher energy efficiency. However, it has a limitation concerning its slow transient response, which has to be considered to avoid premature ageing [21], [22].

In the literature, several studies are presented to propose some EMS strategies for an HPS. Fathabadi et al. [15] proposed a novel FC/SC/battery hybrid system for use in fuel cell hybrid electric vehicles (FCHEVs). The power source consists of a 90-kW proton exchange membrane FC stack, a 19.2 kW lithium-ion battery, and an SC bank of 600 F, which served as a supplementary energy storage device. Ettihir et al. [23] attempted to address EMS for a fuel cell HEVs. Their work focused on the optimal power splitting between the battery pack and the FC, considering the FC's operating conditions.

Xu et al. [24] proposed a multi-objective optimization problem for the powertrain parameters for a pre-defined driving cycle in relation to system durability and fuel economy. Results of their study indicate that the maximal output power of 40 kW for the FC and battery capacity of 150 Ah are optimal for the system durability and fuel economy of a FC city bus in a "Chinese typical city bus drive cycle". Sedaghati and Shakarami [25] also studied a new power and control management strategy for a micro-grid connected to the grid, consisting of a three-phase load and hybrid renewable energy system (HRES). Their hybrid system comprises a PV system SC, a battery storage system (BSS), and a solid oxide fuel cell. Their simulated results showed the effectiveness of an adaptive fractional fuzzy sliding mode control strategy under different loading conditions and various faults. In other studies, Ferahtia et al. [26] worked on a DC microgrid (MG) using an ameliorated power management approach. The study was conducted to provide a management strategy that can guarantee an optimized bus voltage using set power-sharing among the sources. The strategy they proposed decreased the voltage ripple in the DC bus.

Thounthong et al. [27] proposed an EMS for a hybrid system that is made up of a polymer electrolyte membrane fuel cell (PEMFC) and PV array. This included a lithium-ion battery module and SC storage devices. According to their study, they obtained excellent performance using the proposed EMS during load cycles. Carignano et al. [28] considered the FC/SC platform, which constitutes a hard constrained powertrain that delivers an adverse scenario for EMS relative to drivability and fuel economy. They presented a new EMS-based approach for the assessment of short-term future energy demands. Their experimental and simulation results show an enhancement in the consumption of hydrogen and power compliance. Liu and Liu [29] employed Pontryagin's minimum principle to construct a power source sizing model to optimize the battery lifecycle while minimizing fuel consumption, energy loss, and cost of the powertrain. Rodatz et al. [30] presented a full explanation of equivalent consumption minimization (ECM) and their implementation, plus an experimental validation for SC/ FCHV-based power system.

The authors in [31] proposed a new EMS for the SC- battery HPS using optimal adaptive gain LQR- based on the salp swarm algorithm (SSA). This method aims to compute the required gains to obtain the reference power for both SC and battery and then increases the power devices' life expectancies. Another study in [32] was conducted in order to distribute the power demand between the SC and battery energy sources using different strategies, including the proportional-integral (PI) strategy, the external energy maximization strategy (EEMS), and the ECM. As a result, the DC bus voltage is stabilized by the SC which has fast dynamics, while the load power is handled by the battery. The authors in [33] proposed a Total Cost of Ownership (TCO) model that takes into account energy consumption, equivalent energy consumption, and the degradation of various power sources. In that study, the authors implemented the double Q-learning reinforcement learning (RL) algorithm with state

constraints and variable action space in order to identify the most efficient EMS. The authors in [34] proposed a new EMS based on model predictive control (MPC) that combines self-trending prediction and the subset-searching method as a method of applying the best HPS to increase the efficiency of FC and lower the cost of operating FC. The suggested EMS minimizes the inaccuracy of speed forecasting in comparison to the conventional MPC and simplifies the process of calculating the optimum control trajectory, both of which boost the possibility of practical engineering fields. The methodology of RL is becoming an increasingly popular option for the regulation of energy consumption in HPS. Furthermore, the previous work-based EMS for HPS does not place an emphasis on the training environment and the setup of the reward function, and it does not differentiate between the many stages of the development of RL agents. The purpose of the study in [35] is to address this method by first introducing the notion of an RL-based EMS, then providing literature evaluations from both an RL environment and an agent, and then offering some recommendations for future research.

In this study, an EMS is proposed to enhance the efficiency of the HPS powered by battery and SC sources. This strategy is based on the flatness control theory. Flatness control provides excellent performance for nonlinear systems due to the reduced-order model. The performance of this strategy is mainly based on the parameters of the trajectory planning, which are easier to define. The main contributions can be listed in the following:

  i. An efficient EMS ensures a good power quality delivered to the load side and extended HESS device lifetime
  ii. Provides the power reference for both the SC and battery to achieve optimal performance and stable voltage

This paper is organized as follows: Section 2 introduces the hybrid power system configuration. Section 3 highlights the proposed efficient EMS strategy. Section 4 discusses the simulation results and discussion. Section 5 presents the conclusion.

II. HYBRID POWER SYSTEM CONFIGURATION
When the battery is operated with high-frequency loads, the internal resistance may increase, causing the battery to degrade. On the one hand, a high current can be obtained from the battery. On the other hand, the SC has many charging/ discharging cycles and a high-power density. Therefore, using the SC/battery as a HPS can improve the performance and meet the load demand [26], [25]. Several topologies for the HPS are presented, such as passive, semi-active, and full active topologies [26], [31], [32].

In this paper, a fully active SC/battery topology is used as presented in Fig. 1. Both the SC and lithium-ion battery are connected to the DC bus by a bidirectional DC/DC converter to supply the load. In this work, the presented FEMS is based on the flatness control theory that computes the references of the SC and battery to satisfy the DC load demand and maintain the bus voltage with standard limits.
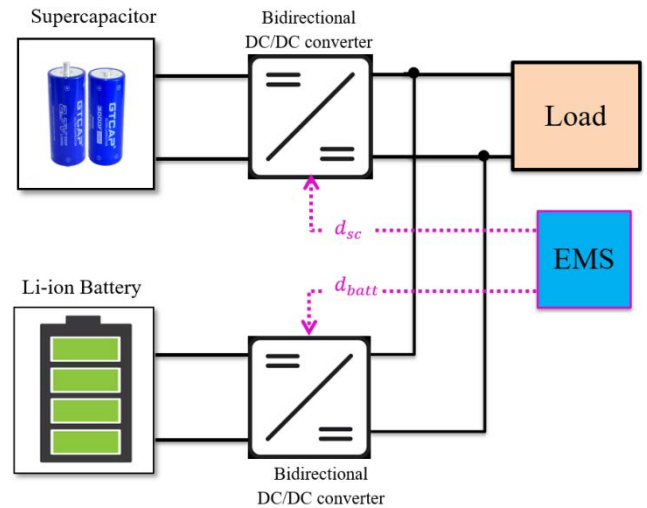

FIGURE 1. Overview of the studied HPS.

A. SUPERCAPACITOR MODELING
A supercapacitor is a high-capacity capacitor used in applications requiring many rapid charge/discharge cycles rather than long-term compact energy storage. It is mainly used for regenerative braking, short-term energy storage, and burst-mode power delivery [27], [30]. In 2016, MathWorks provided a new version of Simulink (2016) that includes a SC model that allows one to quickly show the SC model with its parameters [31]. Therefore, in this paper, the SC model is based on the MATLAB/Simulink, which is reported in Fig. 2. The parameters of this figure can be defined as follows:

- V_{sc} is the terminal voltage of the SC (V).
- i_{SC} is instantaneous current of the SC (A)
- V_c is the controlled voltage-source (V)
- r_{sc} is the internal resistance of SC (Ω)
- Q_T is the supercapacitor electric charge (C).
- A_i is Interfacial area between electrodes and electrolyte (m^2)
- C is molar concentration (mol/m^3)
- F is the Faraday constant
- N_s represent the number of series supercapacitors
- N_e represent the number of layers of electrodes
- N_p is the number of parallel supercapacitors
- d is the molecular radius
- R is the ideal gas constant
- T is the operating temperature (K)
- ε is the permittivity of material
- ε_o is the permittivity of free space

B. LITHIUM BATTERY MODELING
Lithium batteries are widely used in portable consumer electronic devices. It is referred to as a lithium-metal battery with metallic lithium as an anode. Moreover, it stands apart from other batteries in its high charge density and cost per unit [27], [28], [29], [30], [31], [32], [33], [34], [35], [36]. The lithium model used in this research is based on MATLAB/Simulink
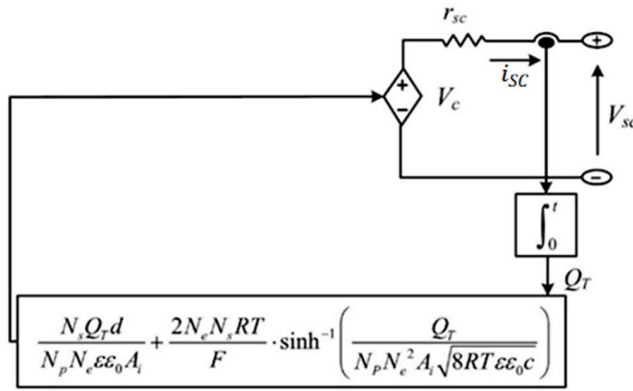
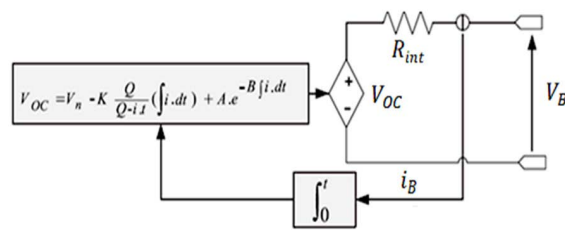**FIGURE 2.** The SC equivalent circuit module.

FIGURE 3. The battery electrical circuit module.

model, as presented in Fig. 3. The parameters of this figure was listed as below:

- R_{int} is the internal resistance of the battery
- V_B is the terminal voltage of the battery (V).
- i_B is instantaneous current of the battery (A)
- V_{OC} is the open-circuit voltage of the battery (V).
- V_n is the nominal voltage of battery (V).
- Q is the battery's capacity (Ah).
- A is the exponential zone amplitude (V).
- B the exponential zonetime constant (Ah^{-1})
- i_t is the current battery charge (Ah).
- K is the polarization constant.

C. LOAD MODELING

The HPS must fulfill the load, whatever its application or type. Most loads are dynamic loads that change with time, such as speed motors in EVs application or load appliances in stationary MG. In this paper, a dynamic load profile based on a controlled current source is used. The required power of the DC load that is connected through the SC and battery has the following formula:

$$P_{load} = i_{load} \cdot v_{bus} \tag{1}$$

where i_{load} is the load current and v_{bus} is the DC bus voltage.

D. DC/DC CONVERTER MODELING

A bidirectional DC/DC converter is used to regulate the charging and discharging procedures of both the SC battery and the Li-ion battery. The use of this converter might result in an improvement to the switching operation, whereby the input current ripple is reduced due to the utilization of

smaller inductor value ranges [37]. As a consequence of this, the conversion stage's efficiency is increased, as are the dynamic capabilities of the storage component (SC) and the battery's safety. By managing the output currents and comparing them with the reference values ($i_{B,ref}$, and $i_{SC,ref}$), the flatness EMS is able to maintain control over the SC as well as the battery. This is accomplished by creating the appropriate duty cycles for the converters. In addition, the bidirectional converter may be dissected based on its two modes of operation—the buck mode and the boost mode—as described in reference [37]. If the converter operates in buck-mode, the input voltage from the battery or the SC will be applied to the inductor. The inductance in this case can be computed as follows:

$$L = \frac{V_{in}(1 - D)}{\Delta i_L f_{sw}} \tag{2}$$

where L is the inductance of the converter, V_{in} is the input voltage of the converter, D is the duty cycle, f_{sw} is the switching frequency, and Δi_L is the ripple in the inductor current. In this scenario, the duty ratio will shift between D_{min} and D_{max} in accordance with the needed value for the DC bus voltage. By controlling this converter, the DC bus voltage can be kept at a constant value that serves as a reference. In addition to this, if the converter was operating in boost mode, the relationship between the voltage of the DC link and the voltage of the input would look like this:

$$v_{bus} = \frac{V_{in}}{(1 - D)} \tag{3}$$

In this case, the input inductor can be calculated from the following equation [37],

$$L = \frac{V_{in} D}{\Delta i_L f_{sw}} \tag{4}$$

III. THE PROPOSED FEMS STRATEGY

A. FLATNESS CONTROL APPROACH

The control scheme may be more difficult under the system's nonlinearity. For this reason, the differential flatness theory was applied to reduce the model's order. As a result, the alternative model enables the dynamics of the trajectories to be characterized based on Fliess et al. [36]. Applying the flatness control theory, the reduced-order model can be formulated as follows [26], [36].

$$y = \phi\left(x, u, \dot{u}, \ldots u^{(\alpha)}\right) \tag{5}$$

$$x = \varphi\left(y, \dot{y}, \ldots y^{(\beta)}\right) \tag{6}$$

$$u = \psi\left(y, \dot{y}, \ldots y^{(\beta+1)}\right) \tag{7}$$

where y is the output flat model, x is the state variable, and u is the control variable. Also, ϕ, φ, and ψ are the functions of the smooth mapping, while $y^{(\beta+1)}$ is the notation for the derivative of the output $(\beta + 1)^{th}$. Also, α is a finite number of the derivative, while $rank(\phi) = m$, $rank(\varphi) = n$, and $rank(\psi) = m$ [26].

B. FLATNESS CONTROL BASED HPS

The flatness control is applied to the SC-battery power system to reduce the order of the model and present the proposed FEMS. As discussed above, the proposed HPS will be defined in Eq.(8).

$$y = \begin{bmatrix} y_1 \\ y_2 \end{bmatrix}, \quad u = \begin{bmatrix} u_1 \\ u_2 \end{bmatrix}, \quad x = \begin{bmatrix} x_1 \\ x_2 \end{bmatrix} \tag{8}$$

By applying this theory to the proposed system, the following equation is defined as

$$y = \begin{bmatrix} E_{bus} \\ E_{SC} \end{bmatrix}, \quad u = \begin{bmatrix} P_{SC\_ref} \\ P_{B\_ref} \end{bmatrix}, \quad x = \begin{bmatrix} v_{bus} \\ v_{SC} \end{bmatrix} \tag{9}$$

The objective of this paper is to control and manage the power-sharing between the SC, battery, and DC load while maintaining the DC bus voltage at the desired value of 400V. As a result, the DC bus energy is controlled by discharging and charging the SC device. Moreover, the capacitive energy for both the DC bus and the SC can be written as [26] and [27]:

$$E_{bus} = \frac{1}{2} C_{bus} v_{bus}^2 \tag{10}$$

$$E_{SC} = \frac{1}{2} C_{SC} v_{SC}^2 \tag{11}$$

where C_{bus} is the DC bus capacitance, C_{SC} the SC capacitance, v_{bus} is the DC bus voltage, and v_{SC} is the instantaneous voltage of the SC. Based on the proposed system configuration, the bus energy E_{bus} can be expressed in function of the power-sharing through the DC bus as follows [26]:

$$\dot{E}_{bus} = P_{SCo} + P_{Bo} - P_{load} \tag{12}$$

where P_{SCo} and P_{Bo} are the transferred power from the SC and battery to the load, respectively, which are can be calculated from Eqs. (13 and 14) as follows:

$$P_{SCo} = P_{SC} - \delta_{SC} \left(\frac{P_{SC}}{v_{SC}} \right)^2 \tag{13}$$

$$P_{Bo} = P_B - \delta_B \left(\frac{P_B}{v_B} \right)^2 \tag{14}$$

where δ_{SC} and δ_B are the SC converter losses and battery converter losses, respectively.

Furthermore, both the SC and battery follow their power reference values which are written as

$$P_{B\_ref} = P_B = v_B i_B \tag{15}$$

$$P_{SC\_ref} = P_{SC} = v_{SC} i_{SC} \tag{16}$$

where and v_B is the instantaneous voltage of the battery. However, the total energy stored in the SC capacitor and DC bus capacitor can be written as [26]

$$E_T = E_{SC} + E_{bus} \tag{17}$$

C. SUPERCAPACITOR AND BATTERY CONTROL LOOP

The SC control scheme depends on the regulation of the total electromagnetic energy. The SC has slower dynamic and enormous capacitive energy over the capacitance of the DC bus [31]. In this work, the SC power reference regulates the voltage of the DC bus and handles the power at a high frequency. The battery supplies power to the load and maintains the SC voltage at the reference value using trajectory planning for the power demand of the SC. The proposed detailed EMS system for both the battery and SC is shown in Fig. 4. However, the state variables of Eqs.(18 and 19) can be expressed as,

$$x_1 = \sqrt{2y_1}/C_{bus} = \phi_1(y_1) \tag{18}$$

$$x_2 = \sqrt{2(y_2 - y_1)}/C_{SC} = \phi_2(y_1, y_1) \tag{19}$$

Furthermore, the first input control represents the SC power reference which can be written from Eqs. (10-19) as,

$$u_1 = P_{SC,ref}$$

$$= 2P_{SC,max} \left[1 - \sqrt{1 - \sqrt{\frac{\dot{y}_1 + \sqrt{\frac{2y_1}{C_{bus}}} \cdot i_{load} - P_{Bo}}{P_{SC,max}}}} \right]$$

$$= \psi_1(\dot{y}_1, y_1) \tag{20}$$

where is the limited maximum power of the SC, $P_{SC,max} = \frac{v_{SC}^2}{4r_{SC}}$.

Moreover, the most important variable in the proposed system is the flat output $y_1 = E_{bus}$. Therefore, a proportional-integral (PI) controller is applied to regulate the dc bus voltage. The SC control loop is considered faster. As a result, the overall power of the HPS in Eq.(21) can be written as

$$\dot{E}_{bus} = P_{SCo} \tag{21}$$

From this equation, the output transfer function is a pure integrator. So, in this work, a PI controller is used based on supposing $y_{1,ref} = E_{bus,ref}$, and the following control equation of DC bus voltage low is expressed as [31],

$$\dot{y}_1 = \frac{1}{s} \left(K_p + \frac{K_i}{s} \right) (y_1 - y_{1,ref}) \tag{22}$$

where $K_p = 2 \cdot \zeta \cdot \omega_n$, $K_i = \omega_n^2$, and ω_n is the natural frequency and ζ is the damping factor.

Furthermore, the control low of the battery used in this paper can be expressed as,

$$\dot{y}_2 - \dot{y}_{2,ref} + K_B(y_2 - y_{2,ref}) = 0 \tag{23}$$

where K_B is the control's gain of the SC controller. The demand power of the SC $(P_{SC,demand})$ is used to generate the trajectory planning based on the following equation,

$$P_{SC,demand} = \left(K_p + \frac{K_i}{s} \right) (y_2 - y_{2,ref}) \tag{24}$$

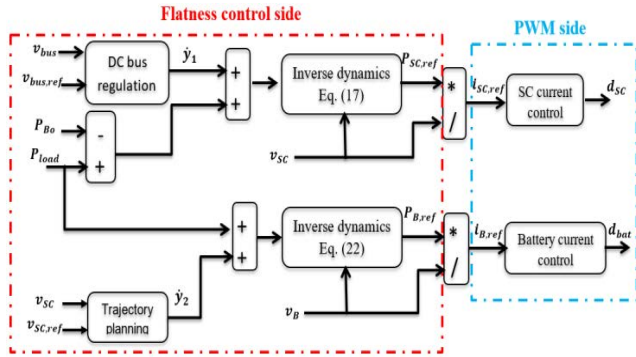Moreover, the second input control represents the battery power reference which can be derivate from Eqs.(1,12,19 and

FIGURE 4. The proposed control loops.

TABLE 1. The proposed system parameters.

Parameter	Value
Reference voltage of the SC, $V_{SC,ref}$	200 V
Reference voltage of the battery, V_b	200 V
Reference voltage of the DC bus, $V_{bus,ref}$	400 V
C_{SC}	120 F
C_{bus}	2200 μF
Q	1500 Ah
L	2 mH
δ_B	0.1
δ_{SC}	0.1
k_p	67
k_i	2500
f_{sw}	25kHz
ω_n	50
ζ	0.67

FIGURE 5. The proposed load power profile.
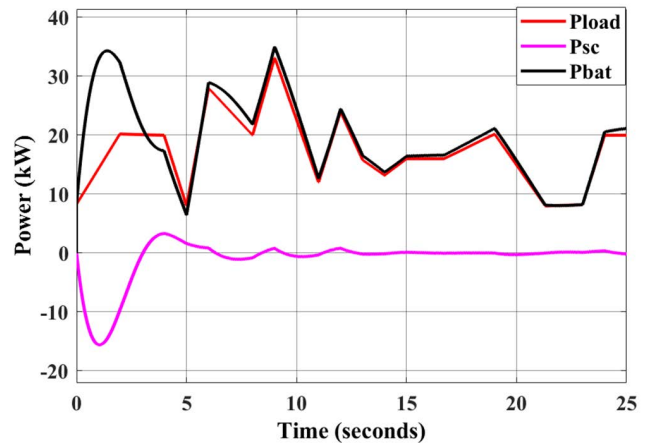
FIGURE 6. The power simulation results.

23) as (25), shown at the bottom of the page, where is the limited maximum power of the battery, $P_{B,max} = \frac{v_B^2}{4r_B}$. Finally, based on the above design, the proposed reduced-order model can be defined as a flat system.

IV. SIMULATION RESULTS AND DISCUSSION

In this work, the proposed EMS is verified using MAT-LAB/Simulink. The parameters of the used system are listed in Table 1. To evaluate and confirm the performance of the proposed energy management strategy, the load power profile with rabid dynamics that is illustrated in Fig. 5 will be used. The simulation time of this profile is 25 seconds. This time is sufficient to evaluate the performance of the HPS with the fast variations of the load power.

The power simulation results are shown in Fig. 6. As observed, the battery takes a large portion of the demand's load. The rapid dynamics of the load can be observed from
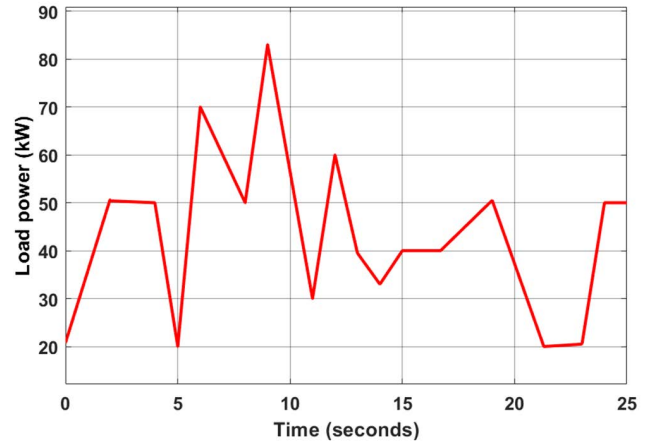
5sec to 15sec. During these times, the maximum power demand of 82kW is seen at time 9sec. This sudden increase in the demand discharges the SC at a rated power of 2kW when the battery is unable to accomplish the increase in the demand load alone. As a result, the load demand is supplied by the battery while the main function of the SC is to handle the transitory load, and this makes the average power zero.

Fig. 8 reports the SC voltage with its reference value. As observed, the SC voltage is controlled by the battery, which maintains a measured voltage at the reference value according to the initial voltage value. Thus, the battery charges the SC based on the trajectory planning to hold its voltage at the reference value. This explains why we propose the use of FEMS.

In addition, the proposed FEMS maintains the DC bus voltage at its reference value (**400V**) during the fast change

$$u_2 = P_{B,ref} = 2P_{B,max} \left[1 - \sqrt{1 - \sqrt{\frac{\dot{y}_{2,ref} + K_B \left(y_{2,ref} - y_2 \right) + \sqrt{\frac{2y_1}{C_{bus}}} \cdot i_{load}}{P_{B,max}}}} \right] = \psi_2 \left(\dot{y}_2, y_1 \right) \quad (25)$$
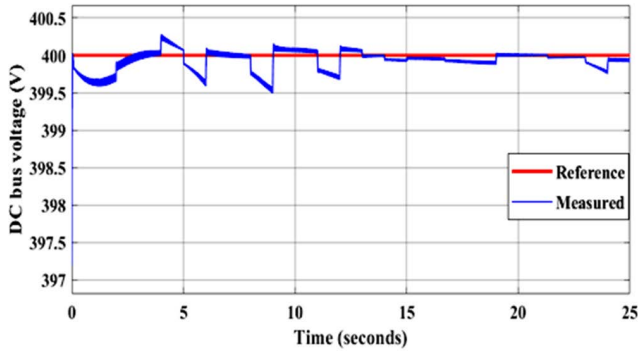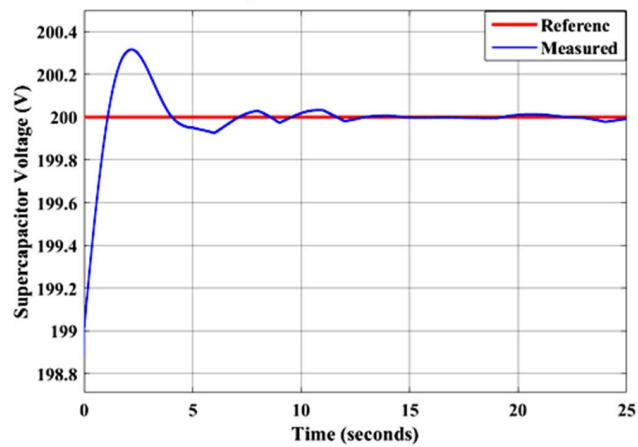
FIGURE 7. The DC bus voltage results.

FIGURE 8. The supercapacitor voltage variations.
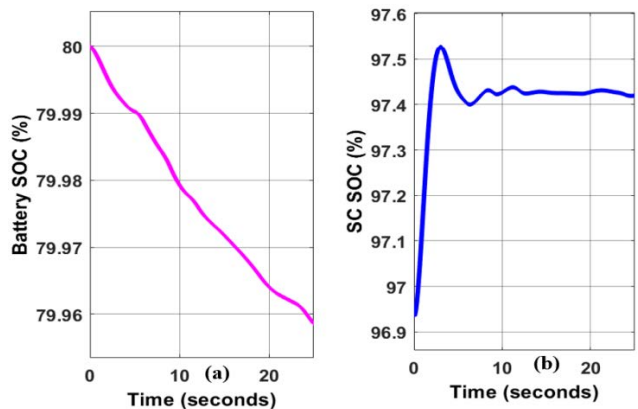
FIGURE 9. The SOC simulation results (a) the SOC of the battery (b) the SOC of the SC.

FIGURE 10. The DC bus voltage results for the proposed and LF strategies.

FIGURE 11. The second power load profile.

in the demand load. Based on the bus voltage control low of the proposed FEMS, the bus voltage is stabilized where the ripple in the voltage is very small, at about $\Delta V = 1V$ as shown in Fig. 7. In addition, the SC voltage with its reference value is illustrated in Fig. 8. Also, the SC is charged by the battery with the initial voltage value of $199\,V$. As a result, the SC will charge itself by negative power amount. Fig. 9 shows the SOC for both the battery and supercapacitor.

To validate the proposed FEMS, the comparison with the classical LF strategy is made under different load conditions. Fig. 10 shows the DC bus voltage at the proposed FEMS and classical LF strategies. As can be seen, the proposed
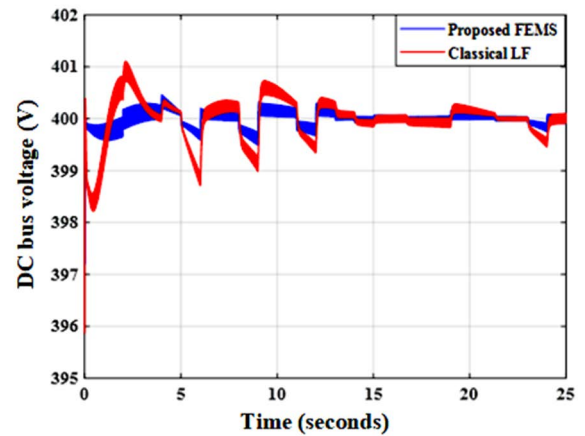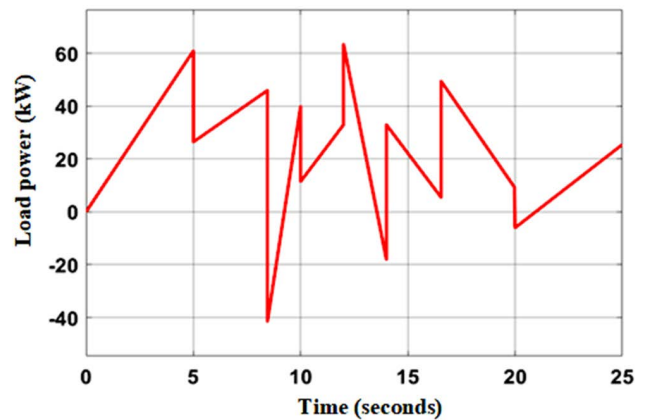
FEMS provides high-quality power under stable operation conditions with minimum overshoot value in the bus voltage. Moreover, the voltage ripple is much lower using the proposed FEMS. Therefore, the performance of the FEMS strategy has improved significantly.

To validate the proposed strategy under both traction and braking cases, the second proposed load power profile is used, as illustrated in Fig. 11, where the power in the traction case is positive and in the braking case becomes negative.

Fig. 12 reports the power simulation results for the second load profile. As seen, the real load is mainly supplied by the battery's power. The supercapacitor provides the transient periods in the load demand, which handles the variations of the load. In the beginning, the battery power is higher than the load and the supercapacitor power is negative. In fact, the battery charges the supercapacitor to raise its SOC (its voltage) to the reference level, as illustrated in Fig. 13. The proposed FEMS has successfully stabilized the bus voltage with high quality, as depicted in Fig. 14. Thus, the proposed strategy successfully maintains the DC bus and supercapacitor voltages with their reference values.

In this load profile, the DC bus voltage is stabilized under fast variations of the load. It is clear that the obtained results confirm the proposed FEMS with high performance
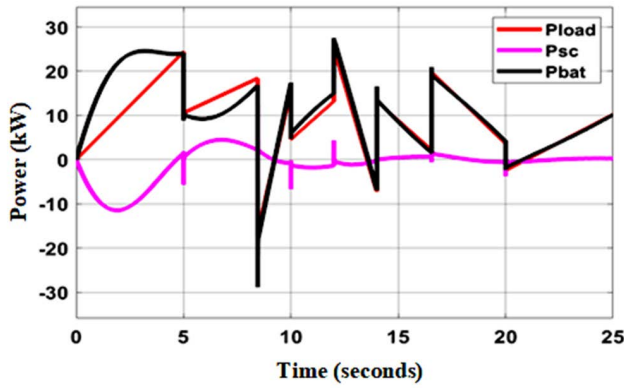
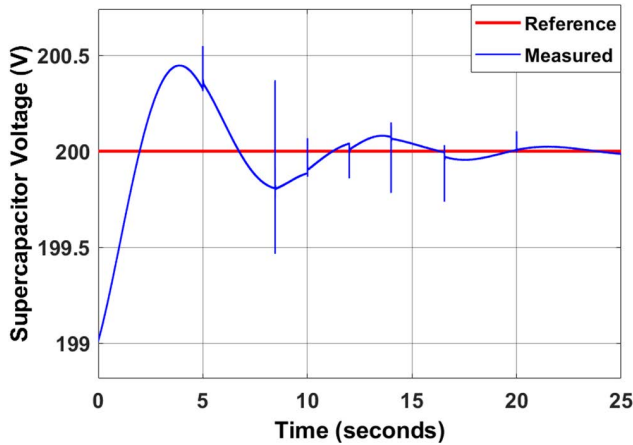**FIGURE 12.** The power simulation results for the second load profile.

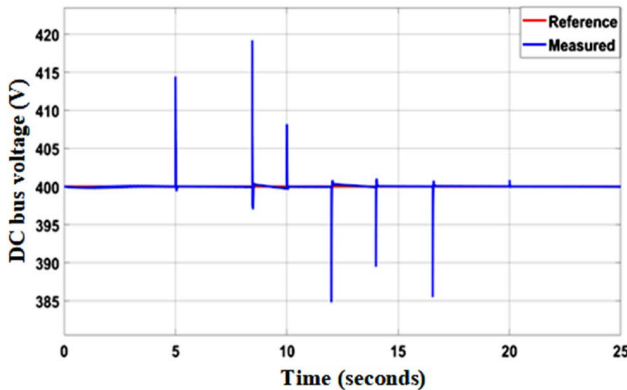**FIGURE 13.** The supercapacitor voltage results.

FIGURE 14. The DC bus voltage results.

FIGURE 15. The DC bus voltage results for the proposed and LF strategies.
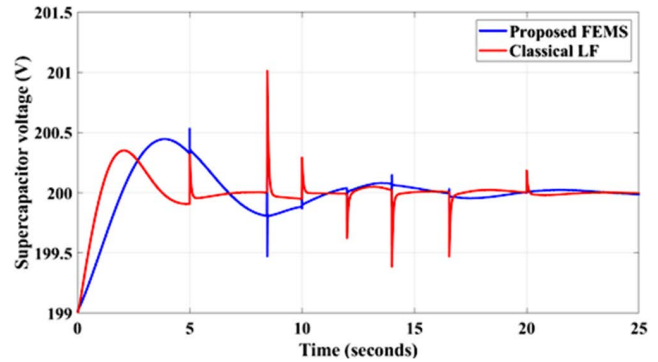
FIGURE 16. The supercapacitor voltage results for the proposed and LF strategies.

TABLE 2. Comparison between the proposed EMS and the conventional LF method.

Parameter	Conventional LF		Proposed FEMS	
$\Delta P_{load}(kW)$	$V_{bus,Peak}$	$V_{SC,Peak}$	$V_{bus,Peak}$	$V_{SC,Peak}$
$0 \to 60$	405	200.4	413	200.5
$46 \to (41.4)$	418	201	<u>419</u>	<u>199.5</u>
$(41.4) \to 40$	403	200.4	408	199.8
$63.5 \to (-18)$	393	199.6	385	200.03
$(-18) \to 33$	<u>375</u>	<u>199.3</u>	402	200.1
$49.5 \to 5.9$	384	200.2	398	200.004

compared with the classical LF control strategy, as shown in Figs. 15 and 16. Moreover, the presented strategy offers high-quality power under variations of the load.

From these obtained results, the proposed FEMS could handle the fast variations in the bus voltage much faster than that of the classic LF. Although the overshoots are slightly larger using the proposed FEMS, the maximum overshoot (6.25%) does not exceed 10% of the reference voltage. Therefore, the proposed FEMS demonstrates its superior high-quality power performance with stable operation. Table 2 demonstrated that the suggested FEMS is better than the
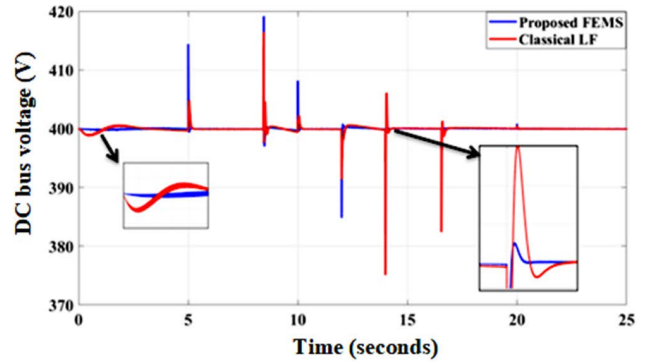
traditional one. As can be observed, the peak voltages for the DC bus and the SC at various demand load variations are represented by $V_{bus,Peak}$ and $V_{SC,Peak}$, respectively, where these values are retrieved from the Figs. 15 and 16. The voltage overshoot is produced with regard to the reference values, where the standard LF shows promising results in the event of moderate variation in demand but fails in the case of quick step demand load. In contrast, the suggested FEMS exhibits good overshoots in bus and SC voltages when the demand is quickly adjusted. The underlined values represent the highest value of $V_{bus,Peak}$ and $V_{SC,Peak}$ for each strategy.

V. CONCLUSION
In this research, a FEMS for a HPS electrified by a supercapacitor battery is presented. The main objective is to provide stable DC bus voltage for the HPS that is composed of a

battery/SC hybrid energy storage system. This paper focuses mainly on stabilizing the DC bus voltage considering the energetic characteristics of the power sources, such as their power dynamics. The battery supplies power to the fundamental load, and the SC regulates the bus power during the transition periods. The EMS is based on a nonlinear differential flatness approach. The flatness provides the system with higher stability and robustness against extreme operating conditions such as fast variations in the load power. The proposed strategy has been evaluated under various conditions. The obtained results confirm its high performance compared with LF control strategy where the voltage stabilization is significantly faster with maximum overshoot near to 6.25%, which indicates the high quality of the provided power. The proposed EMS provides high-quality power with stable operating conditions, and the SC operates with its reference voltage, therefore guaranteeing the enhanced performance of the proposed strategy.

LIST OF NOMENCLATURES

BSS	Battery energy storage
DC	Direct-current
ECM	equivalent consumption minimization
EEMS	external energy maximization strategy
EMS	Energy management strategy
ESS	Energy storage system
EVs	electric vehicles
FC	Fuel cell
FCHEVs	Fuel cell hybrid electric vehicles
FEMS	Flatness energy management strategy
HEVs	hybrid electric vehicles
HFCV	Hydrogen fuel cell vehicle
HPS	Hybrid power system
HRES	Hybrid renewable energy system
LF	Load following
MG	Microgrid
MPC	Model predictive control
PEMFC	polymer electrolyte membrane fuel cell
PI	Proportional-integral
RL	reinforcement learning
SC	Supercapacitor
SOC	State of charge
SSA	Salp swarm algorithm
TCO	Total Cost of Ownership

LIST OF ABBREVIATIONS

u_1	The input control unit
Δi_L	input current ripple
A_i	interfacial area between electrodes and electrolyte (m^2)
C_{SC}	capacitance of the SC (μF)
C_{bus}	capacitance of the DC bus (μF)
E_{SC}	SC capacitive energy (W.sec)
E_T	Total capacitive energy (W.sec)
E_{bus}	DC bus capacitive energy (W.sec)
K_B	gain of the SC charge control

K_i	integral gain
K_p	proportional gain
N_e	number of layers of electrodes
N_p	number of parallel supercapacitors
N_s	number of series supercapacitors
$P_{B,max}$	maximum power of the battery (W)
$P_{B,ref}$	reference power of the battery (W)
P_{Bo}	battery actual power (W)
$P_{SC,demand}$	Demand power of the SC (W)
$P_{SC,max}$	The maximum power of the SC (W)
$P_{SC,ref}$	reference power of the SC (W)
Q_T	supercapacitor electric charge (C).
R_{int}	internal resistance of the battery (Ω)
V_{OC}	open-circuit voltage of the battery (V)
V_c	controlled voltage-source (V)
V_{in}	input voltage (V)
V_n	nominal voltage of battery (V)
V_{sc}	terminal voltage of the SC (V)
f_{sw}	switching frequency (Hz)
i_B	instantaneous value of the Battery current (A)
i_{SC}	instantaneous value of the SC current (A)
i_{load}	Load current (A)
	internal resistance of SC (Ω)
v_B	instantaneous value of the battery voltage (V)
$v_{SC,ref}$	voltage reference of the SC (V)
v_{SC}	instantaneous value of the SC voltage (V)
v_{bus}	instantaneous voltage DC bus (V)
x_1	The state variable of the dc bus
$y^{(\beta+1)}$	Notation for the derivative of the output
y_1	The flat output
δ_B	losses in the battery converter
δ_{SC}	The losses in the SC converter
ε_o	permittivity of free space
τ_1	First order filter gain
ω_n	The natural frequency (rad/sec)
A	exponential zone amplitude (V)
B	exponential zonetime constant (Ah^{-1})
C	molar concentration (mol/m^3)
F	Faraday constant
L	input inductor (mH)
Q	normal battery's capacity (Ah)
R	ideal gas constant
T	operating temperature (K)
d	molecular radius
u	control variable
x	state variable
y	output flat model
α	finite number of the derivative
ε	permittivity of material
ζ	damping factor
$\phi, \varphi,$ and ψ	functions of the smooth mapping
i_t	current battery charge (Ah)
K	polarization constant
D	*duty cycle*

ANNEX

Flat variable generation, first flat variable (v_{bus})

$$E_{bus} = \frac{1}{2}C_{bus}\,v_{bus}^2 \tag{26}$$

$$v_{bus}^2 = 2E_{bus}\big/C_{bus} \tag{27}$$

$$v_{bus} = \sqrt{2E_{bus}\big/C_{bus}} \tag{28}$$

$$x_1 = \sqrt{2y_1\big/C_{bus}} = \phi_1\left(y_1\right) \tag{29}$$

Second flat variable (v_{SC})

$$E_{SC} = \frac{1}{2}C_{SC}v_{SC}^2 \tag{30}$$

$$v_{SC}^2 = 2E_{SC}\big/C_{SC} \tag{31}$$

$$v_{SC}^2 = 2(E_T - E_{bus})\big/C_{SC} \tag{32}$$

$$v_{SC} = \sqrt{2(E_T - E_{bus})\big/C_{bus}} \tag{33}$$

$$v_{SC} = \sqrt{2(y_2 - y_1)\big/C_{SC}} = \phi_2\left(y_1, y_1\right) \tag{34}$$

REFERENCES

[1] E. Vinot and R. Trigui, "Optimal energy management of HEVs with hybrid storage system," *Energy Convers. Manage.*, vol. 76, pp. 437–452, Dec. 2013.

[2] B. Tang, D. Zhang, H. Jiang, and Y. Huang, "Optimization of energy management strategy for the EPS with hybrid power supply based on PSO algorithm," *Energies*, vol. 13, no. 2, p. 428, Jan. 2020.

[3] Y. B. Yu, X. Liu, H. Min, H. Sun, and L. Xu, "A novel fuzzy-logic based control strategy for a semi-active battery/super-capacitor hybrid energy storage system in vehicular applications," *J. Intell. Fuzzy Syst.*, vol. 29, no. 6, pp. 2575–2584, Nov. 2015.

[4] F. Balsamo, C. Capasso, D. Lauria, and O. Veneri, "Optimal design and energy management of hybrid storage systems for marine propulsion applications," *Appl. Energy*, vol. 278, Nov. 2020, Art. no. 115629.

[5] C. Zheng, W. Li, and Q. Liang, "An energy management strategy of hybrid energy storage systems for electric vehicle applications," *IEEE Trans. Sustain. Energy*, vol. 9, no. 4, pp. 1880–1888, Oct. 2018.

[6] P. K. Prasad and P. R. Kumar, "Super twisting algorithm based hybrid energy storage system for electric vehicle," in *Proc. 2nd Int. Conf. Emerg. Technol. (INCET)*, May 2021, pp. 1–7.

[7] R. S. Chandan, T. L. S. Kiran, G. Swapna, and T. V. Muni, "Intelligent control strategy for energy management system with FC/battery/SC," *J. Crit. Rev.*, vol. 7, no. 2, pp. 344–348, 2020.

[8] Y. Sahri, Y. Belkhier, S. Tamalouzt, N. Ullah, R. N. Shaw, M. S. Chowdhury, and K. Techato, "Energy management system for hybrid PV/wind/battery/fuel cell in microgrid-based hydrogen and economical hybrid battery/super capacitor energy storage," *Energies*, vol. 14, no. 18, p. 5722, Sep. 2021.

[9] D. C. Sekhar and M. Manisha, "Energy management control for dual power source powered electric vehicle," *Int. Trans. Elect. Eng. Comput. Sci.*, vol. 2, no. 3, pp. 114–126, Oct. 2021.

[10] R. Wang, D. Hao, Y. Zhang, and X. Meng, "Energy management control of fuel cell electric bus basing on fuzzy rule," *J. Phys., Conf. Ser.*, vol. 2002, no. 1, Aug. 2021, Art. no. 012073.

[11] J. Wu, Z. Wei, K. Liu, Z. Quan, and Y. Li, "Battery-involved energy management for hybrid electric bus based on expert-assistance deep deterministic policy gradient algorithm," *IEEE Trans. Veh. Technol.*, vol. 69, no. 11, pp. 12786–12796, Nov. 2020.

[12] N. Ghadimi, S. Nojavan, O. Abedinia, and A. B. Dehkordi, "Deterministic-based energy management of DC microgrids," in *Risk-Based Energy Management*. New York, NY, USA: Academic, Jan. 2020, pp. 11–30.

[13] D. Yu, T. Zhang, G. He, S. Nojavan, K. Jermsittiparsert, and N. Ghadimi, "Energy management of wind-PV-storage-grid based large electricity consumer using robust optimization technique," *J. Energy Storage*, vol. 27, Feb. 2020, Art. no. 101054.

[14] Z. Fu, L. Zhu, F. Tao, P. Si, and L. Sun, "Optimization based energy management strategy for fuel cell/battery/ultracapacitor hybrid vehicle considering fuel economy and fuel cell lifespan," *Int. J. Hydrogen Energy*, vol. 45, no. 15, pp. 8875–8886, Mar. 2020.

[15] H. Fathabadi, "Novel fuel cell/battery/supercapacitor hybrid power source for fuel cell hybrid electric vehicles," *Energy*, vol. 143, pp. 467–477, Jan. 2018, doi: 10.1016/j.energy.2017.10.107.

[16] M. Frondel, N. Ritter, C. M. Schmidt, and C. Vance, "Economic impacts from the promotion of renewable energy technologies: The German experience," *Energy Policy*, vol. 38, no. 8, pp. 4048–4056, Aug. 2010.

[17] A. Evans, V. Strezov, and T. J. Evans, "Assessment of sustainability indicators for renewable energy technologies," *Renew. Sustain. Energy Rev.*, vol. 13, no. 5, pp. 1082–1088, 2009.

[18] C. Capasso, D. Lauria, and O. Veneri, "Experimental evaluation of model-based control strategies of sodium-nickel chloride battery plus supercapacitor hybrid storage systems for urban electric vehicles," *Appl. Energy*, vol. 228, pp. 2478–2489, Oct. 2018, doi: 10.1016/j.apenergy.2018.05.049.

[19] N. Sulaiman, M. A. Hannan, A. Mohamed, P. J. Ker, E. H. Majlan, and W. R. W. Daud, "Optimization of energy management system for fuel-cell hybrid electric vehicles: Issues and recommendations," *Appl. Energy*, vol. 228, pp. 2061–2079, Oct. 2018, doi: 10.1016/j.apenergy.2018.07.087.

[20] Z. Hu, J. Li, L. Xu, Z. Song, C. Fang, M. Ouyang, G. Dou, and G. Kou, "Multi-objective energy management optimization and parameter sizing for proton exchange membrane hybrid fuel cell vehicles," *Energy Convers. Manage.*, vol. 129, pp. 108–121, Dec. 2016, doi: 10.1016/j.enconman.2016.09.082.

[21] R. Borup et al., "Scientific aspects of polymer electrolyte fuel cell durability and degradation," *Chem. Rev.*, vol. 107, no. 10, pp. 3904–3951, 2007, doi: 10.1021/cr050182l.

[22] S. Strahl, N. Gasamans, J. Llorca, and A. Husar, "Experimental analysis of a degraded open-cathode PEM fuel cell stack," *Int. J. Hydrogen Energy*, vol. 39, no. 10, pp. 5378–5387, Mar. 2014, doi: 10.1016/j.ijhydene.2013.12.115.

[23] K. Ettihir, L. Boulon, and K. Agbossou, "Optimization-based energy management strategy for a fuel cell/battery hybrid power system," *Appl. Energy*, vol. 163, pp. 142–153, Feb. 2016, doi: 10.1016/j.apenergy.2015.10.176.

[24] L. Xu, C. D. Mueller, J. Li, M. Ouyang, and Z. Hu, "Multi-objective component sizing based on optimal energy management strategy of fuel cell electric vehicles," *Appl. Energy*, vol. 157, pp. 664–674, Nov. 2015, doi: 10.1016/j.apenergy.2015.02.017.

[25] R. Sedaghati and M. R. Shakarami, "A novel control strategy and power management of hybrid PV/FC/SC/battery renewable power system-based grid-connected microgrid," *Sustain. Cities Soc.*, vol. 44, pp. 830–843, Jan. 2019, doi: 10.1016/j.scs.2018.11.014.

[26] S. Ferahtia, A. Djerioui, S. Zeghlache, and A. Houari, "A hybrid power system based on fuel cell, photovoltaic source and supercapacitor," *Social Netw. Appl. Sci.*, vol. 2, no. 5, pp. 1–11, May 2020.

[27] P. Thounthong, S. Sikkabut, P. Mungporn, C. Ekkaravarodome, N. Bizon, P. Tricoli, B. Nahid-Mobarakeh, S. Pierfederici, and B. Davat, "Performance investigation of high-energy high-power densities storage devices by li-ion battery and supercapacitor for fuel cell/photovoltaic hybrid power plant for autonomous system applications," in *Proc. IEEE Ind. Appl. Soc. Annu. Meeting*, Oct. 2015, pp. 1–10, doi: 10.1109/IAS.2015.7356844.

[28] M. G. Carignano, R. Costa-Castelló, V. Roda, N. M. Nigro, S. Junco, and D. Feroldi, "Energy management strategy for fuel cell-supercapacitor hybrid vehicles based on prediction of energy demand," *J. Power Sources*, vol. 360, pp. 419–433, Aug. 2017, doi: 10.1016/j.jpowsour.2017.06.016.

[29] C. Liu and L. Liu, "Optimal power source sizing of fuel cell hybrid vehicles based on Pontryagin's minimum principle," *Int. J. Hydrogen Energy*, vol. 40, no. 26, pp. 8454–8464, Jul. 2015, doi: 10.1016/j.ijhydene.2015.04.112.

[30] P. Rodatz, G. Paganelli, A. Sciarretta, and L. Guzzella, "Optimal power management of an experimental fuel cell/supercapacitor-powered hybrid vehicle," *Control Eng. Pract.*, vol. 13, no. 1, pp. 41–53, Jan. 2005, doi: 10.1016/j.conengprac.2003.12.016.

[31] V. Gineste, L. Gajewski, C. Carron, C. Rouzies, A. Marec, and O. Sanchez, "Li-ion battery/supercapacitor hybrid power supply (HPS) for space applications," in *Proc. 10th Eur. Space Power Conf.*, vol. 719. Noordwijkerhout, The Netherlands: ESA Special Publication, Aug. 2014, p. 30.

[32] M. Dhifli, S. Jawadi, A. Lashab, J. M. Guerrero, and A. Cherif, "An efficient external energy maximization-based energy management strategy for a battery/supercapacitor of a micro grid system," *Int. J. Comput. Sci. Netw. Secur.*, vol. 20, no. 1, pp. 196–203, Jan. 2020.

[33] Q. Li, X. Meng, F. Gao, G. Zhang, and W. Chen, "Approximate cost-optimal energy management of hydrogen electric multiple unit trains using double *Q*-learning algorithm," *IEEE Trans. Ind. Electron.*, vol. 69, no. 9, pp. 9099–9110, Sep. 2022.

[34] Q. Li, P. Liu, X. Meng, G. Zhang, Y. Ai, and W. Chen, "Model prediction control-based energy management combining self-trending prediction and subset-searching algorithm for hydrogen electric multiple unit train," *IEEE Trans. Transport. Electrific.*, vol. 8, no. 2, pp. 2249–2260, Jun. 2022.

[35] Q. Li, X. Meng, F. Gao, G. Zhang, W. Chen, and K. Rajashekara, "Reinforcement learning energy management for fuel cell hybrid system: A review," *IEEE Ind. Electron. Mag.*, early access, Feb. 21, 2022, doi: 10.1109/MIE.2022.3148568.

[36] P. R. M. Fliess, J. Levine, and P. Martin, *Systems and Control in the Twenty-First Century*, 1st ed. Boston, MA, USA: Birkhäuser, 1997, p. 22.

[37] H. Wang, S. Dusmez, and A. Khaligh, "Design and analysis of a full-bridge LLC-based PEV charger optimized for wide battery voltage range," *IEEE Trans. Veh. Technol.*, vol. 63, no. 4, pp. 1603–1613, Apr. 2014.

HEGAZY REZK received the B.Eng. and M.Eng. degrees in electrical engineering from Minia University, Egypt, in 2001 and 2006, respectively, and the Ph.D. degree from the Moscow Power Engineering Institute, Moscow. He is an Associate Professor (on leave) with the Electrical Engineering Department, Minia University. He was a Postdoctoral Research Fellow with the Moscow State University of Mechanical Engineering, Russia, for six months. He was a Visiting Researcher with Kyushu University, Japan, for one year. He is currently an Associate Professor with the Electrical Engineering Department, College of Engineering at Wadi Addwaser, Prince Sattam University, Saudi Arabia. He has authored more than 50 technical papers. His research interests include renewable energy, smart grid, hybrid systems, power electronics, optimization, and artificial intelligence.

SALAM J. YAQOOB received the B.Sc. and M.Sc. degrees in electrical power engineering from Middle Technical University, Baghdad, Iraq, in 2014 and 2019, respectively. Since 2015, he has been with the Department of Research and Education, Authority of the Popular Crowd, Prime Minister. He has been active in the field of power electronics and renewable energy, especially in the areas of photovoltaic (PV) systems, energy management systems (EMS), and dc/ac and dc/dc power converters. He has authored more than 23 technical papers in Scopus and Web of Science.

NASEER TAWFEEQ ALWAN received the Bachelor of Refrigeration and Air Conditioning Engineering degree (Hons.) and the Master of Science degree in thermal energy engineering from the Department of Thermal Energy Engineering, Kazan National Research Technical University, Russia, in 2004 and 2014, respectively, and the Doctor of Philosophy degree in renewable energy engineering from Ural Federal University, Russia, in 2021. He is currently working at Northern Technical University, Iraq.

SEYDALI FERAHTIA received the B.Sc. degree in electrical engineering, the M.Sc. degree in automatic systems, and the Ph.D. degree in automatic and industrial computing from the University of M'sila, Algeria, in 2016, 2018, and 2022, respectively. He is currently an Associate Professor at the Department of Electrical Engineering, University of M'sila. His research interests include metaheuristic optimization, hybrid power systems, and hydrogen power systems.

HOSSAM M. ZAWBAA received the B.Sc. and M.Sc. degrees from the Faculty of Computers and Information, Cairo University, Giza, Egypt, in 2008 and 2012, respectively, and the Ph.D. degree from Babeş-Bolyai University, Cluj-Napoca, Romania, in 2018. He is currently an Assistant Professor at the Faculty of Computers and Artificial Intelligence, Beni-Suef University, Beni-Suef, Egypt. He has authored or coauthored over 90 research publications in peer-reviewed reputed journals and international conference proceedings. His research interests include computational intelligence, machine learning, computer vision, and natural language understanding. He has been rated as one of the top 2% scientists worldwide by Stanford in the field of AI, in 2020, 2021, and 2022. Moreover, he has been awarded the State Encouragement Award for the year 2020 in the field of engineering sciences from the Academy of Scientific Research and Technology, Egypt.

ADEL A. OBED received the B.Sc.Eng. degree from the University of Technology, Baghdad, in 1981, and the M.Sc. and Ph.D. degrees in electrical engineering from Basrah University, in 1989 and 2008, respectively. He is a Professor at the Electrical Engineering Department, Middle Technical University, Baghdad. He has published more than 32 papers in different journals and conference proceedings. His research interests include electrical machines control applications, wavelet approach in power and machines systems, and PV applications.

SALAH KAMEL received the joint Ph.D. degree from the University of Jaén, Spain, and Aalborg University, Denmark, in January 2014. He is an Associate Professor with the Electrical Engineering Department, Aswan University. He is also a Leader of the Power Systems Research Group, Advanced Power Systems Research Laboratory (APSR Lab), Aswan, Egypt. His research interests include power systems analysis and optimization, smart grid, and renewable energy systems.

• • •